Neuro-Oncology Advances

3(1), 1–13, 2021 | doi:10.1093/noajnl/vdab056 | Advance Access date 09 April 2021

NBAT1/CASC15-003/USP36 control MYCN expression and its downstream pathway genes in neuroblastoma

Prasanna Kumar Juvvuna, Tanmoy Mondal, Mirco Di Marco, Subazini Thankaswamy Kosalai, Meena Kanduri, and Chandrasekhar Kanduri

Department of Medical Biochemistry and Cell Biology, Institute of Biomedicine, University of Gothenburg, Gothenburg, Sweden (P.K.J., M.D.M., S.T.K., C.K.); Department of Clinical Chemistry and Transfusion Medicine, Sahlgrenska University Hospital, Laboratory Medicine, Institute of Biomedicine, University of Gothenburg, Gothenburg, Sweden (T.M.); Department of Clinical Chemistry and Transfusion Medicine, Sahlgrenska University Hospital, Gothenburg, Sweden (M.K.)

Corresponding Author: Chandrasekhar Kanduri, Department of Medical Biochemistry and Cell Biology, Institute of Biomedicine, University of Gothenburg, 40530 Gothenburg, Sweden (kanduri.chandrasekhar@gu.se).

Abstract

Background. *MYCN* has been an attractive therapeutic target in neuroblastoma considering the widespread amplification of the *MYCN* locus in neuroblastoma, and its established role in neuroblastoma development and progression. Thus, understanding neuroblastoma-specific control of *MYCN* expression at the transcriptional and post-transcriptional level would lead to identification of novel *MYCN*-dependent oncogenic pathways and potential therapeutic strategies.

Methods. By performing loss- and gain-of-function experiments of the neuroblastoma hotspot locus 6p22.3 derived lncRNAs CASC15-003 and NBAT1, together with coimmunoprecipitation and immunoblotting of MYCN, we have shown that both lncRNAs post-translationally control the expression of MYCN through regulating a deubiquitinase enzyme USP36. USP36 oncogenic properties were investigated using cancer cell lines and in vivo models. RNA-seq analysis of loss-of-function experiments of CASC15-003/NBAT1/MYCN/USP36 and JQ1-treated neuroblastoma cells uncovered *MYCN*-dependent oncogenic pathways.

Results. We show that NBAT1/CASC15-003 control the stability of MYCN protein through their common interacting protein partner USP36. *USP36* harbors oncogenic properties and its higher expression in neuroblastoma patients correlates with poor prognosis, and its downregulation significantly reduces tumor growth in neuroblastoma cell lines and xenograft models. Unbiased integration of RNA-seq data from *CASC15-003*, *NBAT1*, *USP36*, and *MYCN* knockdowns and neuroblastoma cells treated with *MYCN* inhibitor JQ1, identified genes that are jointly regulated by the *NBAT1*/*CASC15-003*/*USP36*/*MYCN* pathway. Functional experiments on one of the target genes, *COL18A1*, revealed its role in the *NBAT1*/*CASC15-003*-dependent cell adhesion feature in neuroblastoma cells.

Conclusion. Our data show post-translational regulation of *MYCN* by *NBAT1*/*CASC15-003*/USP36, which represents a new regulatory layer in the complex multilayered gene regulatory network that controls *MYCN* expression.

Key Points

- Post-translational control of MYCN expression by sense-antisense lncRNAs CASC15/NBAT1.
- NBAT1/CASC15/MYCN/USP36/COL18A1 controlled novel oncogenic pathway in neuroblastoma.

Importance of the Study

MYCN amplification and its expression have served as reliable biomarkers in the stratification of neuroblastoma risk status. Hence, there is a greater appreciation in the neuroblastoma research community in understanding the mechanisms that control *MYCN* oncogene expression at the transcriptional and post-transcriptional levels, and also, in characterizing the novel MYCN-dependent downstream oncogenic pathways to devise potential therapeutic opportunities for the treatment of high-risk NBs. In this investigation, we show that *NBAT1* and *CASC15-003* lncRNAs regulate *MYCN* expression post-translationally through their interacting protein partner USP36, which is a deubiquitinating enzyme. Our study also characterizes the *NBAT1*/*CASC15-003*/*MYCN*/USP36/ *COL18A1*-controlled oncogenic pathway in neuroblastoma pathogenesis.

Neuroblastoma (NB), a tumor of neural crest origin, is the most common extracranial solid tumor. It typically develops from sympathetic ganglia in the abdomen, the majority of which develop from adrenal medulla.[1,2] It is the second most common solid tumor after central nervous system tumors affecting children. Being a complex disease, patients are classified into low-, intermediate-, or high-risk groups based on a set of well-defined prognostic indicators such as age of diagnosis, segmental chromosomal aberrations, and stage of the disease.[3,4]

In NB, nonrandom segmental chromosomal aberrations are considered well-defined prognostic markers in the clinical setting, with implications in therapeutic decision strategy. For example, chromosome alterations such as 1p deletion, 11q deletion, 17q gain, and *MYCN* oncogene amplification are routinely used in therapeutic decision strategy.[5,6] Interestingly, about 25% of NB cases show *MYCN* gene amplification, which is a well-characterized chromosomal alteration. *MYCN* gene amplification is associated with aggressive and highly metastatic NB, and confers dismal prognosis and poor survival.[7,8] Aggressive NBs with the *MYCN* gene amplification (MNA) have <50% survival rates with a higher frequency of relapse of the disease, which poses a challenge to rigorous therapeutic procedures. The MYCN protein belongs to the 3-member MYC family of oncoproteins that also includes c-MYC and l-MYC. Unlike the ubiquitously expressed *c-MYC*, *MYCN* expression is confined to the embryonic nervous system and mesenchymal tissue. Moreover, *MYCN* expression is reduced in adult tissues and differentiated neurons.[9,10] *MYCN* is implicated in a wide range of biological functions associated with cancer development and progression, including pluripotency, self-renewal, proliferation, metastasis, and angiogenesis.[8] Experimental overexpression of *MYCN* promotes tumor phenotypes in vitro and in vivo,[11,12] further reinforcing its role in oncogenesis. *MYCN* expression is regulated at the transcriptional[13,14] and post-transcriptional level[15–18] through cooperation between transcriptional factors and long noncoding RNAs (lncRNAs). In addition to the elevated levels of *MYCN* RNA, the stability of the MYCN protein also plays a vital role in NB.[19–21] However, the mechanisms by which lncRNAs control *MYCN* protein stability, and their role in *MYCN*-dependent oncogenic pathways, remain poorly investigated.

Advanced high-throughput sequencing technologies enabled identification of thousands of lncRNAs in the human transcriptome. LncRNAs are encoded by the RNA pol II enzyme, are typically >200 nucleotides in size with little or no coding potential and are widely implicated in the regulation of biological processes linked to cancer. Previously, a genome-wide association study identified three NB-specific risk-associated SNPs within chromosome locus 6p22.3, including the most significantly associated SNP rs6939340. NB patients carrying the homozygous risk allele G (G/G) at the rs6939340 SNP show *MYCN* amplification and are most likely to develop high-risk and metastatic disease. Interestingly, our differential expression analysis of low-risk and high-risk NB tumors revealed some of the top differentially expressed lncRNAs, such as *NBAT1* and *CASC15-003*, which map to the 6p22.3 region. *NBAT1* and *CASC15-003* are NB-specific tumor suppressors that show lower expression in NB patients with *MYCN* amplification.[22,23] In this study, we wanted to investigate the functional connection between *NBAT1*/*CASC15-003* and *MYCN*-dependent oncogenic pathways.

Materials and Methods

Cell Lines

SH-SY5Y, IMR-32, and Kelly cells were purchased from CLS Cell Lines Service. SK-N-BE2 cells were obtained from DSMZ, German Collection of Microorganisms and Cell Cultures GmbH. Cell lines used in this study were maintained at 37°C with 5% CO_2 and cultured in respective media as per manufacturer's instructions.

Plasmid Constructs

For details, please refer to Supplementary Materials and Methods.

Transient Transfections

For details, please refer to Supplementary Materials and Methods.

Generation of Stable Knockdown Cells

Lentiviral shRNA particles targeting *CASC15-003* and *NBAT1*, *USP36*, and non-target shRNA control were purchased from Sigma-Aldrich and stable shRNA cells were generated using a method described previously.[22,23]

Co-immunoprecipitation

Co-immunoprecipitation was performed as described previously[23] except for a few modifications. Cells were lysed in BC100 buffer (20 mM Tris-HCl pH 7.9, 100 mM NaCl, 10% Glycerol, 0.2 mM EDTA, 0.1% Triton X-100, fresh protease inhibitor) and 5 µg of anti-MYCN antibody was added and incubated at 4°C overnight on a rotor. Next day antibody:lysate mixture was incubated with ProteinA, magnetic beads for 1 h at 4°C. Beads were washed thrice in BC100 buffer and the bead bound antibody:protein complexes were analyzed by Western blot.

Immunoprecipitation of Ubiquitinated Proteins

Immunoprecipiation to detect the ubiquitination of endogenous or ectopically expressed MYCN in MG132 (15 µM for 15 h) treated cells was perfromed as described previously.[23] Unlike cultured cells, xenografts were not treated with MG132 and instead MG132 was added to the IP lysis buffer in which the tumors were homogenized using a glass mortar and pestle. Lysates were harvested from the homogenized tissue by centrifugation at 14,000 rpm for 30 min at 4°C. IP was performed with respective antibodies followed by immunoblotting to analyze the ubiquitination status using FK2 antibody (anti-ubiquitin antibody).

Immunoblot

For details, please refer to Supplementary Materials and Methods.

Immunofluorescence

For details, please refer to Supplementary Materials and Methods.

Proliferation Assay

Please refer to Supplementary Materials and Methods for details.

Cell Adhesion Assay

Cell adhesion assay was performed as described previously.[24] In brief, cell culture plates were coated with 15 µg/mL of bovine collagen 1 (Cat# A1064401, Thermofisher scientific) for at least 2 h at room temperature. Collagen solution was then removed and the plates were allowed to dry for about 1 h before seeding the cells. Twenty-five thousand cells were seeded and allowed to settle for 30 min in a cell incubator. The unattached cells were removed and the adherent cells were gently washed a couple of times with 1× PBS. The adherent cells were then estimated by performing MTT assay using CellTiter 96 Non-Radioactive Cell Proliferation assay kit from Promega (G4000) as per manufacturer's instructions.

Colony Formation Assay

For details, please refer to Supplementary Materials and Methods.

Wound Healing Assay

Please refer to Supplementary Materials and Methods for details.

Xenografts in Mice

Xenografts in 5- to 6-week-old Bagg Albino (inbred research mouse strain) nude mice (n = 4) with control or USP36Sh KD IMR-32 cells were generated as described previously.[23] All the mouse experiments were approved by the Animal Ethical Review Board, University of Gothenburg, Gothenburg, Sweden (Ethical permit number-5.8.18-02708/2017).

Chromatin Immunoprecipitation (ChIP)

For details, please refer to Supplementary Materials and Methods.

Differential Gene Expression Analysis

Please refer to Supplementary Materials and Methods for details.

Statistical Analysis

P values were calculated using Student's *t*-test or analysis of variance where statistical significance was represented as (*) *P*-value ≤ .05, (**) *P*-value ≤ .01, (***) *P*-value ≤ .001. (*) *P*-value ≤ .05 is considered significant.

Results

6p22.3 lncRNAs CASC15-003 and NBAT1 Regulate MYCN Protein Levels in NB Via USP36

6p22.3 lncRNAs *CASC15-003* and *NBAT1* show higher expression in low-risk NBs compared to the high-risk patients, and their higher levels in NB patients predicts better clinical outcome. *MYCN* amplification in NB patients, on the other hand, predicts worse prognosis and is often associated with metastasis and relapse. *MYCN* amplified (MNA) tumors have low *CASC15-003* and *NBAT1* compared to the

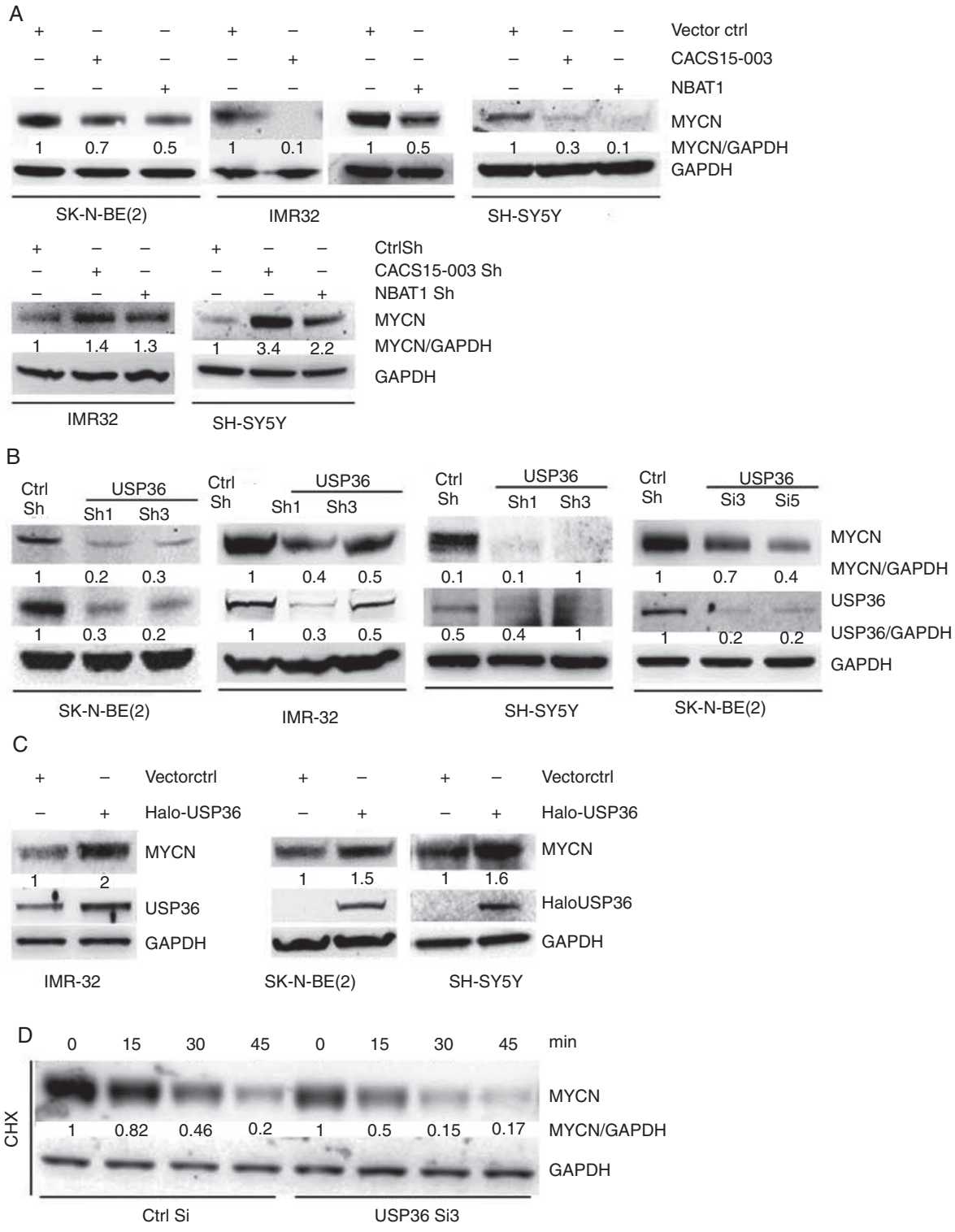

Figure 1. 6p22.3 lncRNAs *CASC15-003* and *NBAT1* regulate MYCN levels in neuroblastoma (NB) cells. (A) Immunoblot shows the MYCN protein levels in vector control, *CASC15-003* and *NBAT1* overexpressing SK-N-BE(2), IMR-32, and SH-SY5Y cells (upper panel) and in Ctrl Sh, *CASC15-003* and *NBAT1* shRNA transduced IMR-32 and SH-SY5Y cells (lower panel). Vector control and Ctrl Sh were used as controls for overexpression and KD, respectively. GAPDH is used as a loading control. (B) Immunoblot of MYCN and USP36 in *USP36* KD SK-N-BE(2), IMR-32, and SH-SY5Y cells. KD was carried out using lentiviral shRNA particles in SK-N-BE(2), IMR-32, and SH-SY5Y, whereas transient *USP36* KD was performed using siRNA in SK-N-BE(2) (last panel on the right). Ctrl Sh or Ctrl Si was used as a control and GAPDH as a loading control. (C) Immunoblot of MYCN and

MYCN nonamplified (nonMNA) ones.[22,23] This intrigued us to check for the abundance of these RNAs and their connection to MYCN protein levels in MNA and non-MNA cell lines. For this, we examined the expression levels of 6p22.3 lncRNAs in MNA cell lines (IMR-32, SK-N-BE(2) and KELLY) and non-MNA cell lines (NB69 and SH-SY5Y). In line with the tumor data, MNA cell lines showed reduced expression of *CASC15-003* and *NBAT1* as compared to the non-MNA cell lines (Supplementary Figure S1A). This inverse correlation between *CASC15-003*/*NBAT1* expression and MYCN protein levels encouraged us to probe the functional connection between MYCN and *CASC15-003*/*NBAT1* in NB. Toward this end, we analyzed MYCN protein levels following loss- and gain-of-function assays for these 2 lncRNAs. Overexpression of *CASC15-003* or *NBAT1* in SK-N-BE(2), IMR-32 and SH-SY5Y cell lines resulted in reduced MYCN protein levels (Figure 1A, upper panel), whereas shRNA mediated knockdown (KD) of these 2 lncRNAs in IMR-32 and SH-SY5Y led to an increase in MYCN protein levels (Figure 1A, lower panel). KD of *CASC15-003* or *NBAT1* could not be achieved in SK-N-BE(2) as the endogenous abundance of these two RNAs is quite low (Supplementary Figure S1A). On the other hand, *MYCN* mRNA levels were not altered significantly in SK-N-BE(2) cells overexpressing the 2 lncRNAs (Supplementary Figure S1B). These findings suggest that *MYCN* is not regulated at the transcriptional level by *CASC15-003* and *NBAT1*, but rather at the post-translational level.

LncRNAs are indeed known to regulate the stability and abundance of their target proteins by direct or indirect mechanisms. Previous studies identified ubiquitin-specific protease USP36 as a common interacting protein partner of *CASC15-003* and *NBAT1,* and these lncRNAs control USP36 activity through modulating its spatial organization.[23] USP36 was shown to deubiquitinate target proteins to determine their stability.[23,25,26] C-MYC, a member of the MYC family of proteins, was shown to be stabilized by the deubiquitinase activity of USP36.[26,27] Considering that MYCN is a paralogue of c-MYC, we sought to investigate if USP36 could regulate MYCN protein levels through its deubiquitinase activity. To test this hypothesis, *USP36* was stably downregulated in SK-N-BE(2), IMR-32, and SHSY5Y cell lines by transduction of 2 independent short hairpin RNAs (shRNAs). In addition, transient KD of *USP36* was performed in SK-N-BE(2) cells using siRNA. Both stable and transient *USP36* KD led to reduced levels of MYCN protein (Figure 1B). As expected, *USP36* overexpression in SK-N-BE(2), IMR-32, and SHSY5Y cells resulted in an increase in MYCN protein levels (Figure 1C). These results strongly suggest that USP36 positively regulates MYCN protein levels. However, *MYCN* RNA levels were not affected following KD or overexpression of *USP36* (Supplementary Figure S1C), suggesting a post-transcriptional regulation of *MYCN* by USP36, most probably through regulating MYCN ubiquitination levels. We tested the stability of the MYCN protein in *USP36* siRNA KD cells by a cycloheximide chase experiment. A striking reduction in the MYCN protein was observed in *USP36* KD cells in comparison to the control cells (Figure 1D), suggesting that USP36 determines the stability of MYCN through post-transcriptional regulation.

USP36 Interacts With MYCN and Regulates Its Stability by Deubiquitination

To understand the role of USP36 in regulating MYCN protein stability, we sought to investigate the interaction between these 2 proteins by immunocytochemistry. Endogenous MYCN and USP36 co-localize with the nucleolar-specific protein NPM1 in IMR-32 cells (Figure 2A). Also, Halo-USP36 and HA-MYCN showed co-localization when overexpressed in SH-SY5Y (Figure 2B). To further investigate the interaction between USP36 and MYCN, we performed a co-immunoprecipitation (Co-IP) of MYCN to verify its association with USP36 in SK-N-BE(2) and IMR-32 cell lines. We found that endogenous MYCN interacts with USP36 in both of the cells lines (Figure 2C, left and middle panels). Consistent with the endogenous MYCN and USP36 interaction data, ectopically expressed Halo-USP36 was immunoprecipitated with the endogenous MYCN in HeLa cells, further confirming the interaction between MYCN and USP36 (Figure 2C, right panel).

Considering that the ubiquitin-specific protease USP36 enhances the stability of target proteins through the removal of ubiquitin moieties, we thought USP36 interaction with MYCN could be involved in the regulation of MYCN stability via ubiquitin mediated proteasomal degradation. We first confirmed the presence of MYCN in the ubiquitinated protein pool by immunoprecipitation with the ubiquitin targeting FK2 antibody (Figure 2D, upper panel). We next verified the role of USP36 in the maintenance of MYCN ubiquitination status by overexpressing both MYCN and USP36. We found that ubiquitination of ectopic MYCN was lower in cells that overexpress USP36 compared to cells overexpressing MYCN alone (Figure 2D, lower panel), indicating that USP36 is a deubiquitinating enzyme for MYCN. To address this further, we tested the ubiquitination status of the endogenous MYCN protein following *USP36* loss-of-function and gain-of-function experiments. *USP36* KD using shRNAs revealed a significant increase in ubiquitinated MYCN levels (Figure 2E, upper panel), whereas its overexpression led to decreased accumulation of ubiquitinated MYCN (Figure 2E, lower panel). Similarly, *USP36*Sh KD xenografts also showed higher MYCN ubiquitination as compared to the control tumors (Supplementary Figure

USP36 in SK-N-BE(2), IMR-32, and SH-SY5Y, where *USP36* was overexpressed from Halo-USP36 plasmid. Vector ctrl was used as a control and GAPDH as a loading control. (D) Immunoblot of MYCN protein levels in cycloheximide chase experiment. SK-N-BE(2) cells transfected with control or USP36 siRNA followed by treatment with cycloheximide (50 µg/mL) and harvested at the given time intervals. The values indicate the fold change in MYCN protein levels normalized to GAPDH. Ctrl Si was used as a control and GAPDH as a loading control for the immunoblot. (A–C) Immunoblots for MYCN in non-MNA SH-SY5Y cells were always exposed longer as compared to MNA cells for the detection of MYCN protein. The values indicate fold change in protein levels of MYCN or USP36 normalized to GAPDH.

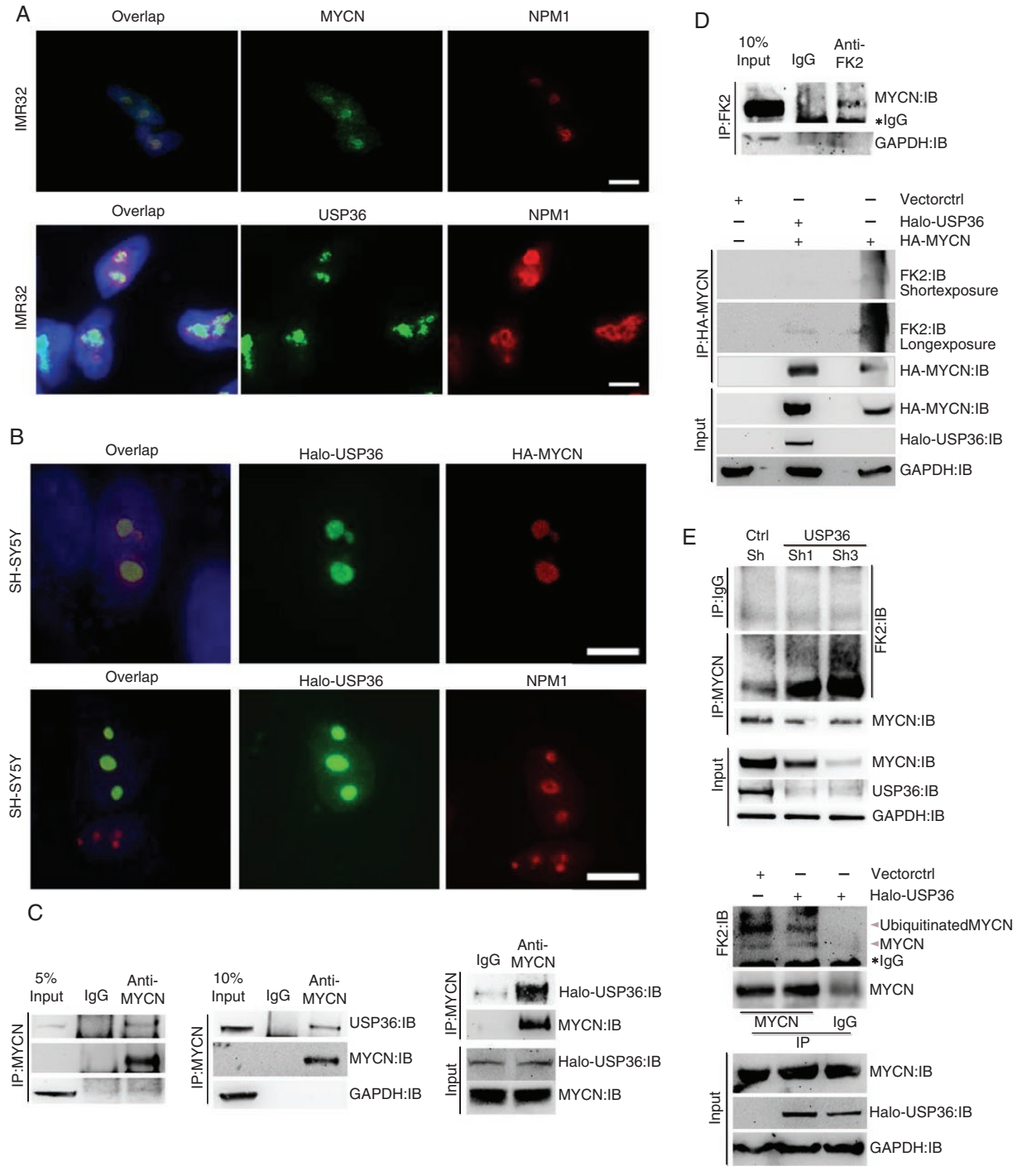

Figure 2. USP36 interacts with and regulates MYCN protein. (A) Upper panel: Immunostaining analysis in IMR-32 cells shows the endogenous MYCN in green and nucleolar marker nucleophosmin (NPM1) in red, stained with anti-MYCN and anti-NPM1 antibodies, respectively. DAPI was used as the nuclear stain. Lower panel: Immunostaining of USP36 (green) and NPM1 (red) stained with anti-USP36 and anti-NPM1 antibodies, respectively, in IMR-32 cells. DAPI was the nuclear stain. Scale bar, 5 μm. (B) SH-SY5Y cells transiently transfected with Halo-USP36 and HA-MYCN expressing plasmids followed by immunostaining analysis. Upper panel: Immunostaining of Halo-USP36 and HA-MYCN stained with anti-Halo and anti-HA antibodies, respectively. DAPI was the nuclear stain. Lower panel: Immunostaining for Halo-USP36 and NPM1 stained with anti-Halo or anti-NPM1 antibodies, respectively. DAPI was the nuclear stain. Scale bar, 5 μm. (C) Co-immunoprecipitation (Co-IP) showing the interaction between MYCN and USP36. Left and middle panels show the endogenous MYCN immunoprecipitation using anti-MYCN antibody in SK-N-BE(2) and IMR-32 cells, respectively. Anti-MYCN and anti-USP36 antibodies detected the presence of MYCN and USP36 in the anti-MYCN immunoprecipitation, IP:MYCN (lane3 from left). Left and middle lanes represent 5 or 10% input and negative control IgG, respectively. GAPDH immunoblot rules out the

S1D). These results indicate that USP36 interacts with and deubiquitinates MYCN, thereby promoting the stability of MYCN.

USP36 Promotes NB Cell Proliferation and Tumor Phenotype

To understand the role of *USP36* in NB pathogenesis, we tested the effect of *USP36* KD on cell proliferation, colony formation, and tumor growth in xenograft models. Depletion of *USP36* by shRNA in SK-N-BE(2) and IMR-32 resulted in a decrease in cell proliferation (Figure 3A) and reduced colony formation (Figure 3B). The tumorigenic potential of *USP36* was tested in xenografts, where stable *USP36*Sh KD IMR-32 cells were subcutaneously injected into nude mice. Depletion of *USP36* significantly reduced the tumor weight, tumor volume and Ki67 staining, indicating that *USP36* harbors oncogenic properties (Figure 3C and D).

Integrated Transcriptome Analyses Identify Common Target Genes Regulated by CASC15-003, NBAT1, USP36, and MYCN

Our findings indicate that the 6p22.3 locus-derived lncRNAs *CASC15-003* and *NBAT1* can determine cell proliferation and tumorigenesis in NB by regulating MYCN stability via modulating USP36 function. To further understand how the functional interplay between *CASC15-003*/*NBAT1*/USP36 and MYCN control NB pathogenesis, we performed transcriptomic analysis following the individual KD of *CAC15-003*, *NBAT1*, *USP36,* and *MYCN*. We also performed RNA-seq on NB cells treated with JQ1, a transcriptional inhibitor of *MYCN*. Specifically, since *NBAT1*/*CASC15* are tumor suppressors, and *USP36*/*MYCN* oncogenic functions are gained in *CASC15*/*NBAT1* KD cells, we therefore compared upregulated genes from *CASC15*/*NBAT1* KD RNA-seq data[22,23] with downregulated genes from RNA-seq datasets obtained from *USP36 KD*/*MYCN KD*/JQ1 treated cells (Supplementary Tables 1–3). These integrated transcriptomic analyses identified four jointly regulated target genes, *COL18A1*, *EGFL7*, *ITGB5*, and *OAF* (Figure 4A and B), which show significant deregulation in the transcriptomic data from all 4 KDs as well as the JQ1 treatment (Figure 4B–D). We further validated the expression of the four genes using RT-qPCR following KD of *CASC15-003*, *NBAT1*, *MYCN*, and *USP36*, as well as in the JQ1 treated cells (Figure 4E–H). *COL18A1*, *EGFL7*, *ITGB5*, and *OAF* showed significant upregulation after *NBAT1* and *CASC15-003* KD (Figure 4E), whereas they were downregulated in the *MYCN* KD, *USP36* KD, and JQ1-treated samples (Figure 4F–H, Supplementary Figure S1E). These results suggest that *COL18A1*, *EGFL7*, *ITGB5*, and *OAF* genes are part of a *CASC15-003*/*NBAT1*/MYCN/USP36 controlled regulatory network.

COL18A1 Contributes to the *MYCN*-Dependent Tumor Phenotype in NB Cells

The *COL18A1* gene encodes alpha chain of type XVIII collagen, which is an extracellular matrix protein.[28–30] Hence, we became particularly interested in understanding the functional role of *COL18A1* in the context of *CASC15-003*/*NBAT1*/USP36/MYCN regulated pathways. We first investigated whether *COL18A1* is directly regulated by MYCN. For this, we overexpressed *MYCN* in *USP36* siRNA KD SK-N-BE(2) cells. *COL18A1* expression was rescued in *MYCN* overexpressed cells compared to *USP36* KD cells (Figure 5A). To further confirm the direct regulation of *COL18A1* by *MYCN*, chromatin immunoprecipitaion (ChIP) with MYCN antibody was performed in *CASC15-003* and *NBAT1* depleted SH-SY5Y cells. The ChIP assays on *CASC15-003* and *NBAT1* depleted cells showed increased MYCN occupancy at the *COL18A1* promoter compared with the control cells (Figure 5B). Since COL18A1 is an extracellular matrix protein, we investigated its role in wound healing, cell proliferation and extra cellular matrix organization in SK-N-BE(2) cells. siRNA-mediated KD of *COL18A1* significantly reduced the wound healing efficiency (Figure 5C) and the cell proliferation rate (Figure 5D) of SK-N-BE(2) cells. *COL18A1* KD also affected the cell adhesion efficacy of SK-N-BE(2) cells (Figure 5E, left panel). Interestingly, we found an increase in the cell adhesion

non-specific interactions in the Co-IP. Right panel: shows interaction between ectopically expressed MYCN and USP36 in HeLa cells. MYCN and Halo-USP36 were ectopically expressed in HeLa cells and the lysates were subjected to immunoprecipitation with anti-MYCN antibody in IP:MYCN. Anti-MYCN and anti-Halo antibodies detected the presence of MYCN and USP36 in both IP:MYCN and input. IgG is the negative control for IP. (D) Ubiquitination of MYCN in NB cells. Upper panel: Immunoblot shows the presence of MYCN in lysates (lane 3) immunoprecipitated with anti-FK2 antibody in SK-N-BE(2) cells treated overnight with MG132, IP:FK2. IgG used as a negative control and GAPDH immunoblot served as a control for nonspecific binding. Lower panel: Ectopically expressed Halo-USP36 deubiquitinates HA-MYCN in HeLa cells. HA-MYCN and Halo-USP36 were ectopically expressed in Hela cells. Two days after transfection, cells were treated with MG132 overnight and subjected to IP with anti-HA antibody. Immunoblot shows the ubiquitinated HA-MYCN in IP:HA-MYCN detected by FK2 antibody. IP:HA-MYCN also shows the levels of immunoprecipitated HA-MYCN. Anti-HA, Anti-Halo and Anti-GAPDH detect the levels of ectopic MYCN, USP36 and endogenous GAPDH, respectively. (E) Immunoblot for ubiquitinated MYCN in USP36 stable KD or USP36 overexpressing SK-N-BE(2) cells. Cells were treated with MG132 overnight and MYCN was immunoprecipitated and analyzed by Immunoblot to check the ubiquitination status of MYCN. Upper panel: Lysates from IMR-32 cells, stably transduced with Ctrl or *USP36*Sh1 and Sh3, were immunoprecipitated with anti-MYCN antibody. Immunoblot shows the ubiquitination of immunoprecipitated MYCN in IP:MYCN detected by FK2 antibody. Also, IP:MYCN shows the levels of immunoprecipitated MYCN. Anti-MYCN, anti-USP36, and anti-GAPDH antibodies detect the MYCN, USP36, and GAPDH levels, respectively, in IP:MYCN and Input. IgG is the negative control for IP. Lower panel: MYCN was immunoprecipitated from HeLa cells, ectopically expressing vector Ctrl or Halo-USP36. Immunoblot shows the ubiquitinated MYCN detected by FK2 antibody and the corresponding levels of MYCN detected by anti-MYCN antibody in IP:MYCN. Anti-Halo, anti-MYCN and anti-GAPDH antibodies detect the levels of Halo-USP36, MYCN, and GAPDH, respectively, in the input.

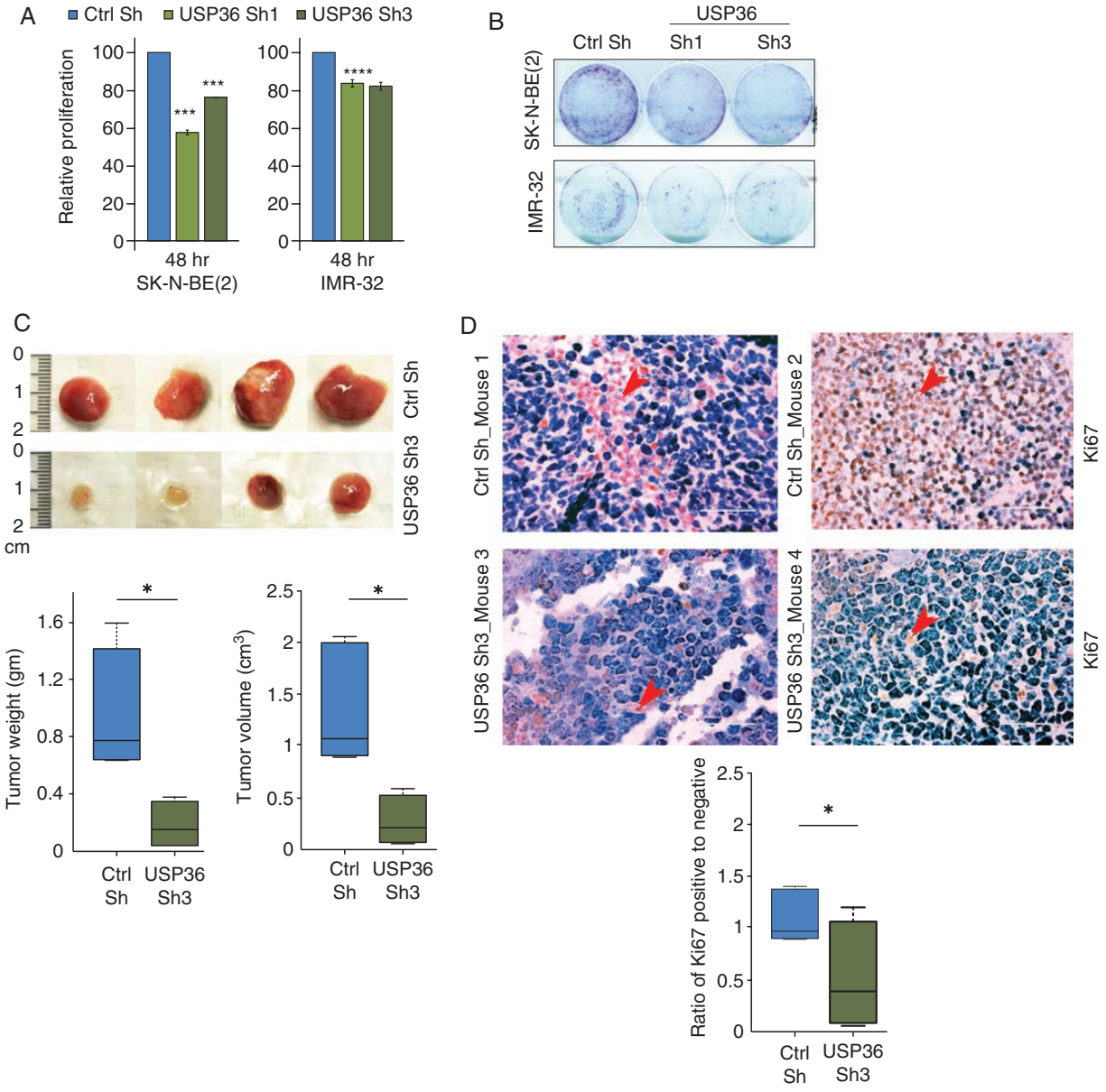

Figure 3. USP36 KD promotes tumor suppression. (A) MTT assay represents the proliferation status of IMR-32 and SK-N-BE(2) cells stably transduced with Ctrl or *USP36*Sh1 and Sh3. Equal number of Ctrl or *USP36Sh* cells were seeded and allowed to proliferate for 48 h and then MTT assay was performed. (B) Representative images of the colony formation assay in IMR-32 and SK-N-BE(2) cells stably transduced with Ctrl or *USP36*Sh1 and Sh3. Equal number of Ctrl or *USP36Sh* cells were seeded and Colony formation assay was performed 5 days after plating. (C,D) IMR-32 cells stably transduced with ctrl or *USP36*ShRNA were subcutaneously injected to develop xenografts in mice. Tumors were harvested 40 days postinjection in mice. (C) Upper panel: Representative images of the tumors depicting the tumor size from xenografts ($n = 4$). Lower panel: Box plots indicate the average weight (left) and volume (right) of the tumors from the upper panel. (D) Upper panel: representative images of the Ki67 staining on the xenografts derived from stable Ctrl or *USP36*Sh3 IMR-32 cells. Short arrow heads indicate the representative Ki67-positive cells. Scale bar, 50 μm. Lower panel: Box plot shows the percentage of Ki67-positive cells counted from 3 different fields in Ctrl or *USP36*Sh3 xenografts. For box plots (C and D), middle line represents the median and the box limits are 25th and 75th percentiles, whiskers are nearer quartile ± 1.5 times interquartile range. For A, C, and D, values represent mean +SD. *$P < .05$, **$P < .01$, and ***$P < .001$ by Student's *t*-test (2-tailed, 2-sample unequal variance).

efficacy of *CASC15-003* and *NBAT1* KD cells (Figure 5E, middle panel) and this increased cell adhesion was lost following *COL18A1* KD (Figure 5E, right panel). Taken together, our data indicate that *COL18A1* plays an important role in *CASC15-003*/*NBAT1*/USP36/MYCN controlled extracellular matrix organization in NB.

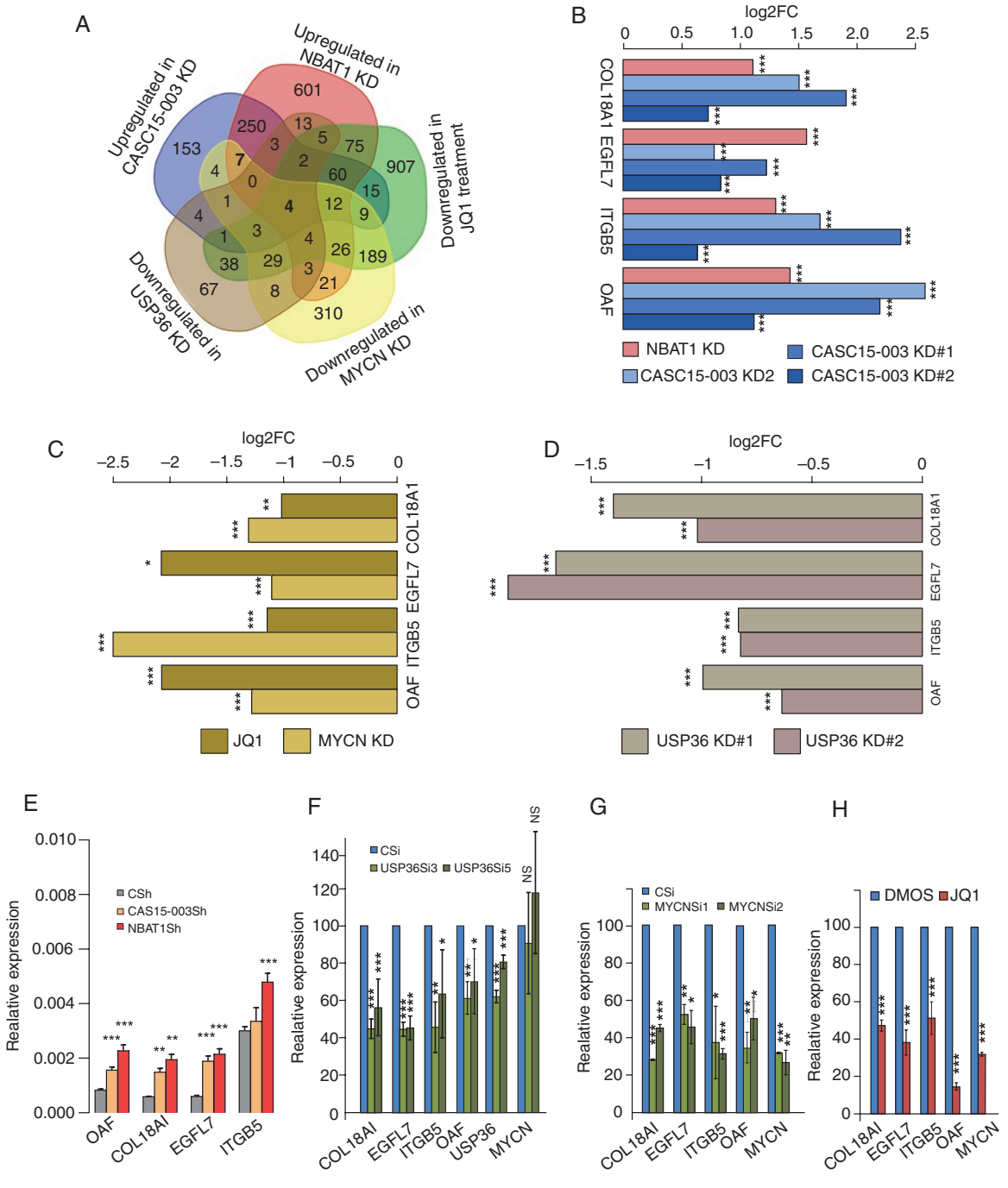

Figure 4. Transcriptome analysis to identify common targets between CASC15-003, NBAT1, USP36, and MYCN. (A) Venn diagram showing the overlap of downregulated genes from *USP36* KD, *MYCN* KD and JQ1-treated SK-N-BE(2) cells with upregulated genes from *CASC15-003* and *NBAT1* KD SH-SY5Y cells. (B) Bar graph showing the fold change of common genes (Figure 4A) in *NBAT1* and *CASC15-003* KD SH-SY5Y cells. (C) Bar graph showing fold change of common genes (Figure 4A) in *MYCN* KD and JQ1-treated SK-N-BE(2) cells. The significances are indicated by $*P < .05$, $**P < .01$, and $***P < .001$. (D) Bar graph showing fold change of common genes (Figure 4A) in *USP36* KD SK-N-BE(2) cells. (E–H) Expression analysis of target genes *COL18A1, EGFL7, OAF,* and *ITGB5* by RT-qPCR. (E) RT-qPCR analysis of *COL18A1, EGFL7, OAF,* and *ITGB5* in SH-SY5Y cells stably KD for CASC15-003 and NBAT1. (F) SK-N-BE(2) cells were transiently transfected with control siRNA or USP36 siRNA3 and USP36 siRNA5 for 48 h followed by RNA extraction and RT-qPCR. Bar graph represents the expression of *COL18A1, EGFL7, ITGB5, OAF, USP36,* and *MYCN.* (G) SK-N-BE(2) cells transiently were transiently transfected with Control siRNA or MYCN siRNA1 and MYCN siRNA2 for 48 h and then expression of *COL18A1, EGFL7, OAF ITGB5,* and *MYCN* genes was analyzed by RT-qPCR. (H) Bar graph represents the relative expression of *COL18A1, EGFL7, OAF, ITGB5,* and *MYCN* mRNA in SK-N-BE(2) cells treated with vehicle control DMSO or JQ1 for 14 h. (B–H) The significances are indicated by $*P < .05$, $**P < .01$, and $***P < .001$.

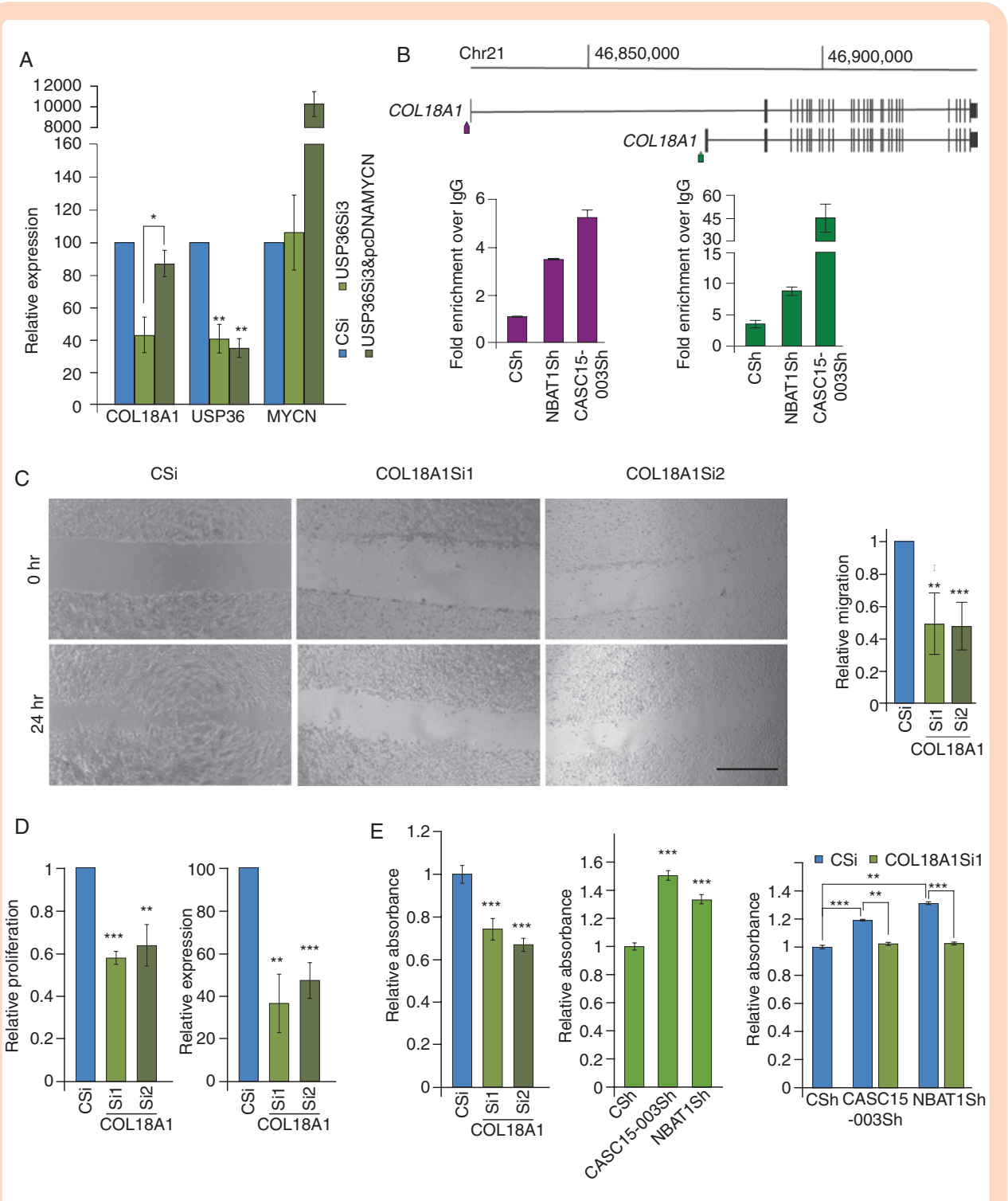

Figure 5. *COL18A1* contributes to extracellular matrix organization in neuroblastoma. (A) qPCR analysis of *COL18A1* showing the rescue of *COL18A1* expression in SH-SY5Y cells. *COL18A1* following USP36 KD/MYCN overexpression compared to the cells transfected with USP36SiRNA or CSi. (B) Schematic showing the exonic structure of the *COL18A1* gene with purple and green pointers indicating the MYCN binding sites on the *COL18A1* promoters. ChIP-qPCR shows the occupancy of MYCN at the promoters of *COL18A1* isoforms in stable CSh or *NBAT1*Sh and *CASC15-003*Sh SH-SY5Y cells. (C) Wound healing assay depicting the cell migration potential in *COL18A1* KD SK-N-BE(2) cells. Cells were transiently transfected with Csi or *COL18A1* siRNA 1 and 2 for 36 h followed by making a scratch on the monolayer. The initial (0 h) and final (24 h) wound lengths were measured, and relative migration was plotted as a bar graph on the right. Scale bar represents 500 μM. (D) Proliferation assay depicts the relative proliferation status of SK-N-BE(2) transfected with Csi or *COL18A1* siRNA 1 and 2. MTT assay was performed 48 h post-transfection to determine the relative proliferation, left panel. Bar graph represents the relative expression of *COL18A1* in Csi

Discussion

Nearly half of the high-risk NB patients harbor *MYCN* amplification and display poor clinical outcome with metastatic dissemination and increased risk of relapse. Since *MYCN* is a critical oncogenic driver in NB pathogenesis, there is an increasing appreciation for understanding MYCN driven downstream oncogenic pathways, and also upstream pathways that control MYCN expression at the transcriptional, post-transcriptional and post-translational level. Previous studies have demonstrated the role of protein coding RNAs in the regulation of MYCN-dependent oncogenic pathways. However, not much has been learnt on the role of lncRNAs in *MYCN* dependent oncogenic pathways. Nevertheless, a few recent investigations have shown that lncRNAs such as *MYCNOS* and *LncUSMycN*, both of which are located in the vicinity of the *MYCN* gene, regulate *MYCN* at the transcriptional and post-transcriptional level. For example, *MYCNOS* lncRNA regulates *MYCN* expression either by altering the usage of *MYCN* promoters or by activating *MYCN* transcription by directly recruiting CTCF to the *MYCN* promoter. *MYCNOS* has also been shown to act as an mRNA, encoding the NCYM protein which is implicated in MYCN stability, On the other hand, *LncUSMycN* interacts with the spliceosome complex protein NONO and stabilizes *MYCN* transcript. Although these studies reveal functional connections between lncRNAs and *MYCN* transcriptional and post-transcriptional regulation, the molecular mechanisms by which lncRNAs control the MYCN dependent oncogenic pathways are lacking.

In this investigation, we demonstrate that the NB hotspot locus derived lncRNAs *NBAT1* and *CASC15-003* regulate *MYCN* expression post-translationally through the regulation of the deubiquitinating enzyme USP36. Both *NBAT1* and *CASC15-003* lack any sequence homology, yet they jointly regulate *MYCN* expression post-translationally via the ubiquitin-proteosome system. Post-translational regulation of *MYCN* by *NBAT1*/*CASC15-003*/USP36 represents a new regulatory layer in the complex multilayered gene regulatory network that controls *MYCN* expression. Another interesting aspect of the current investigation is the demonstration of *USP36* as an oncogene. Its higher expression in NB patients correlates with poor prognosis,[23] and its downregulation significantly reduces tumor growth in cultured cancer cells and xenograft models. These observations coupled with the published literature on *NBAT1*, *CASC15-003* and *MYCN* indicate that, in the *NBAT1*/*CASC15-003*/USP36/MYCN regulatory axis, *NBAT1*/*CASC15-003* serve as tumor suppressors, whereas *MYCN* and *USP36* behave as oncogenes, and that the functional interplay between *NBAT1*/*CASC15-003* and *USP36*/*MYCN* may contribute to NB pathogenesis.

This investigation also characterizes novel *MYCN*-dependent pathways in the NB context. These novel MYCN-dependent pathways were obtained following an unbiased integration of RNA-seq datasets from *CASC15-003*, *NBAT1*, *USP36*, and *MYCN* knockdowns and NB cells treated with the *MYCN* inhibitor JQ1. The integrated RNA-seq analysis revealed four genes, *COL18A1*, *EGFL7*, *ITGB5*, and *OAF*. Among the 4 genes, *COL18A1* is an interesting candidate considering its role in the organization of the extracellular matrix, and closure of the neural tube and brain development which are closely connected to NB development and progression.[31,32] In vitro cell culture assays revealed that *COL18A1* knockdown interferes with cell migration, cell proliferation and cell adhesion. Its ability to rescue the increased cell adhesion property of the *NBAT1*/*CASC15-003* KD cells suggests that *COL18A1* may play an important role in *MYCN* dependent tumor phenotype.

COL18A1, which encodes human collagen XVIII protein, is a widely expressed proteoglycan in the basement membrane. It generates three isoforms with varied N terminal regions and a conserved C-terminal region that encodes an angiogenic inhibitor, endostatin.[33] Human collagen XVIII protein shows higher expression in many solid tumors.[34–37] Its higher expression in stromal cells is associated with metastatic activity.[38,39] Lower expression of *COL18A1* was also observed in several cancers[38,40–42] and this in particular is consistent with endostatin antitumorigenic and antiangiogenic properties.[43,44] These observations indicate that *COL18A1* possesses both oncogenic and tumor suppressor properties in a context dependent manner. *COL18A1* expression dependence on the *NBAT1*/*CASC15-003*/*USP36*/*MYCN* regulatory axis indicates that it may possess oncogenic properties. *NBAT1*/*CASC15-003* play a crucial role in the regulatory axis through modulating the activity of deubiquitinase USP36, leading to the enhanced stability of MYCN. Interestingly, both MYCN and USP36 are colocalized in the nucleolus and show endogenous interaction. The stabilization of MYCN in turn activates *COL18A1*, thereby increasing cell migration and cell adhesion properties. These observations indicate that the *NBAT1*/*CASC15-003*/USP36/MYCN/ *COL18A1* regulatory axis may have crucial role in metastatic activity in high-risk NB patients. However, the higher expression of *COL18A1* in certain tumors correlates with increased overall and event-free survival, including for NB.[40] If one considers the tumor suppressor properties of *COL18A1* in certain tumors together with antiangiogenic and antitumorigenic properties of its cleaved product endostatin, it might give us the impression that higher *COL18A1* expression in tumors may help in tumor regression or sensitize tumors to chemotherapy. The latter contention is consistent with the fact that *MYCN* expressing tumors are more sensitive to chemotherapy than nonexpressing tumors.[45,46] Furthermore, *COL18A1* shows higher expression in stage 4S NB tumors compared to the other INSS stages (Supplementary Figure

or *COL18A1* siRNA1 and 2 KD cells, right panel. (E) Bar graphs represent the effect of *COL18A1* on cell adhesion potential in SK-N-BE(2) and SH-SY5Y cells. SK-N-BE(2) cells were transfected with Csi or *COL18A1* siRNA 1 and 2 for 48 h followed by trypsinization, plating and allowed to adhere for 30 min. Adherent cells were measured by MTT assay, left panel. SH-SY5Y cells with stable KD of *CASC15-003* and *NBAT1* were transfected with Csi or *COL18A1* siRNA 1 for 48 h followed by cell adhesion assay as detailed above, right panel.

S1F), and 4S stage tumors with higher metastatic activity are prone to tumor regression. Thus, we speculate that the *NBAT1/CASC15-003*/USP36/MYCN/*COL18A1* regulatory axis may help in the tumor regression of high-risk 4S NB tumors. Alternatively, this regulatory axis may take part in higher metastatic activity. Further work is warranted to distinguish the oncogenic and/or tumor suppressor functions of *COL18A1* in the context of the *NBAT1/CASC15-003*/USP36/MYCN regulatory axis.

Supplementary Material

Supplementary material is available at *Neuro-Oncology Advances* online.

Keywords

long noncoding RNA | neuroblastoma | USP36 | MYCN | COL18A1 | CASC15 | NBAT1

Acknowledgments

The computations for RNA-sequencing datasets were performed on resources provided by the Uppsala Multidisciplinary Center for Advanced Computational Science (UPPMAX) high-performance computing (HPC) which is part of the Swedish National Infrastructure for Computing (SNIC). We thank Jennifer Uhler, University of Gothenburg, for help with the manuscript editing.

Funding

This work was supported by grants from Knut and Alice Wallenberg Foundation [KAW2014.0057]; Swedish Cancer Research foundation [Cancerfonden: Kontrakt no. CAN2018/591]; Swedish Research Council [2017–02834]; Barncancerfonden [PR2018-0090]; Ingabritt och Arne Lundbergs forskningsstiftelse (LU2020-0017) and LUA/ ALF (to C.K.) and Assar Gabrielssons Fond FB-18-10 (to P.K.J.).

Conflicts of interest statement. Authors do not have any conflicts of interest to declare.

Authorship Statement. C.K. and P.K.J. conceptualized the study, wrote the manuscript, P.K.J. performed co-immunoprecipitations, functional experiments and analyzed data, T.M. performed immunostaining, and performed functional experiments, M.D.M. performed functional experiments on COL18A1, S.T.K. performed bioinformatic analysis, and M.K. performed ChIP-qPCR analysis.

References

1. Maris JM. Recent advances in neuroblastoma. *N Engl J Med.* 2010;362(23):2202–2211.
2. Tsubota S, Kadomatsu K. Origin and initiation mechanisms of neuroblastoma. *Cell Tissue Res.* 2018;372(2):211–221.
3. Pinto NR, Applebaum MA, Volchenboum SL, et al. Advances in risk classification and treatment strategies for neuroblastoma. *J Clin Oncol.* 2015;33(27):3008–3017.
4. Aygun N. Biological and genetic features of neuroblastoma and their clinical importance. *Curr Pediatr Rev.* 2018;14(2):73–90.
5. Mueller S, Matthay KK. Neuroblastoma: biology and staging. *Curr Oncol Rep.* 2009;11(6):431–438.
6. Van Arendonk KJ, Chung DH. Neuroblastoma: tumor biology and its implications for staging and treatment. *Children (Basel).* 2019;6(1).
7. Brodeur GM, Seeger RC, Schwab M, Varmus HE, Bishop JM. Amplification of N-myc in untreated human neuroblastomas correlates with advanced disease stage. *Science.* 1984;224(4653):1121–1124.
8. Huang M, Weiss WA. Neuroblastoma and MYCN. *Cold Spring Harb Perspect Med.* 2013;3(10):a014415.
9. Zimmerman KA, Yancopoulos GD, Collum RG, et al. Differential expression of myc family genes during murine development. *Nature.* 1986;319(6056):780–783.
10. Stanton BR, Perkins AS, Tessarollo L, Sassoon DA, Parada LF. Loss of N-myc function results in embryonic lethality and failure of the epithelial component of the embryo to develop. *Genes Dev.* 1992;6(12A):2235–2247.
11. Weiss WA, Aldape K, Mohapatra G, Feuerstein BG, Bishop JM. Targeted expression of MYCN causes neuroblastoma in transgenic mice. *EMBO J.* 1997;16(11):2985–2995.
12. Cheng AJ, Cheng NC, Ford J, et al. Cell lines from MYCN transgenic murine tumours reflect the molecular and biological characteristics of human neuroblastoma. *Eur J Cancer.* 2007;43(9):1467–1475.
13. Suenaga Y, Kaneko Y, Matsumoto D, Hossain MS, Ozaki T, Nakagawara A. Positive auto-regulation of MYCN in human neuroblastoma. *Biochem Biophys Res Commun.* 2009;390(1):21–26.
14. Zhao X, Li D, Pu J, et al. CTCF cooperates with noncoding RNA MYCNOS to promote neuroblastoma progression through facilitating MYCN expression. *Oncogene.* 2016;35(27):3565–3576.
15. Chen CY, Shyu AB. AU-rich elements: characterization and importance in mRNA degradation. *Trends Biochem Sci.* 1995;20(11):465–470.
16. Gu L, Zhang H, He J, Li J, Huang M, Zhou M. MDM2 regulates MYCN mRNA stabilization and translation in human neuroblastoma cells. *Oncogene.* 2012;31(11):1342–1353.
17. Manohar CF, Short ML, Nguyen A, et al. HuD, a neuronal-specific RNA-binding protein, increases the in vivo stability of MYCN RNA. *J Biol Chem.* 2002;277(3):1967–1973.
18. Claeys S, Denecker G, Durinck K, et al. ALK positively regulates MYCN activity through repression of HBP1 expression. *Oncogene.* 2019;38(15):2690–2705.
19. Otto T, Horn S, Brockmann M, et al. Stabilization of N-Myc is a critical function of Aurora A in human neuroblastoma. *Cancer Cell.* 2009;15(1):67–78.
20. Suenaga Y, Islam SM, Alagu J, et al. NCYM, a Cis-antisense gene of MYCN, encodes a de novo evolved protein that inhibits GSK3β resulting in the stabilization of MYCN in human neuroblastomas. *PLoS Genet.* 2014;10(1):e1003996.
21. Tavana O, Li D, Dai C, et al. HAUSP deubiquitinates and stabilizes N-Myc in neuroblastoma. *Nat Med.* 2016;22(10):1180–1186.

22. Pandey GK, Mitra S, Subhash S, et al. The risk-associated long noncoding RNA NBAT-1 controls neuroblastoma progression by regulating cell proliferation and neuronal differentiation. *Cancer Cell*. 2014;26(5):722–737.
23. Mondal T, Juvvuna PK, Kirkeby A, et al. Sense-antisense lncRNA pair encoded by locus 6p22.3 determines neuroblastoma susceptibility via the USP36-CHD7-SOX9 regulatory axis. *Cancer Cell*. 2018;33(3):417–434 e417.
24. Russo MA, Paolillo M, Sanchez-Hernandez Y, et al. A small-molecule RGD-integrin antagonist inhibits cell adhesion, cell migration and induces anoikis in glioblastoma cells. *Int J Oncol*. 2013;42(1):83–92.
25. Geisler S, Jäger L, Golombek S, et al. Ubiquitin-specific protease USP36 knockdown impairs Parkin-dependent mitophagy via downregulation of Beclin-1-associated autophagy-related ATG14L. *Exp Cell Res*. 2019;384(2):111641.
26. Liu Q, Sheng W, Ma Y, et al. USP36 protects proximal tubule cells from ischemic injury by stabilizing c-Myc and SOD2. *Biochem Biophys Res Commun*. 2019;513(2):502–508.
27. Sun XX, He X, Yin L, Komada M, Sears RC, Dai MS. The nucleolar ubiquitin-specific protease USP36 deubiquitinates and stabilizes c-Myc. *Proc Natl Acad Sci USA*. 2015;112(12):3734–3739.
28. Muragaki Y, Timmons S, Griffith CM, et al. Mouse Col18a1 is expressed in a tissue-specific manner as three alternative variants and is localized in basement membrane zones. *Proc Natl Acad Sci USA*. 1995;92(19):8763–8767.
29. Halfter W, Dong S, Schurer B, Cole GJ. Collagen XVIII is a basement membrane heparan sulfate proteoglycan. *J Biol Chem*. 1998;273(39):25404–25412.
30. Saarela J, Rehn M, Oikarinen A, Autio-Harmainen H, Pihlajaniemi T. The short and long forms of type XVIII collagen show clear tissue specificities in their expression and location in basement membrane zones in humans. *Am J Pathol*. 1998;153(2):611–626.
31. Utriainen A, Sormunen R, Kettunen M, et al. Structurally altered basement membranes and hydrocephalus in a type XVIII collagen deficient mouse line. *Hum Mol Genet*. 2004;13(18):2089–2099.
32. Caglayan AO, Baranoski JF, Aktar F, et al. Brain malformations associated with Knobloch syndrome--review of literature, expanding clinical spectrum, and identification of novel mutations. *Pediatr Neurol*. 2014;51(6):806–813 e808.
33. Heljasvaara R, Aikio M, Ruotsalainen H, Pihlajaniemi T. Collagen XVIII in tissue homeostasis and dysregulation—Lessons learned from model organisms and human patients. *Matrix Biol*. 2017;57-58:55–75.
34. Guenther U, Herbst H, Bauer M, et al. Collagen type XVIII/endostatin is differentially expressed in primary and metastatic colorectal cancers and ovarian carcinomas. *Br J Cancer*. 2001;85(10):1540–1545.
35. Balasubramanian SP, Cross SS, Globe J, Cox A, Brown NJ, Reed MW. Endostatin gene variation and protein levels in breast cancer susceptibility and severity. *BMC Cancer*. 2007;7:107.
36. Väänänen A, Ylipalosaari M, Parikka M, et al. Collagen XVIII modulation is altered during progression of oral dysplasia and carcinoma. *J Oral Pathol Med*. 2007;36(1):35–42.
37. Karppinen SM, Honkanen HK, Heljasvaara R, et al. Collagens XV and XVIII show different expression and localisation in cutaneous squamous cell carcinoma: type XV appears in tumor stroma, while XVIII becomes upregulated in tumor cells and lost from microvessels. *Exp Dermatol*. 2016;25(5):348–354.
38. Musso O, Theret N, Heljasvaara R, et al. Tumor hepatocytes and basement membrane-Producing cells specifically express two different forms of the endostatin precursor, collagen XVIII, in human liver cancers. *Hepatology*. 2001;33(4):868–876.
39. Hu TH, Huang CC, Wu CL, et al. Increased endostatin/collagen XVIII expression correlates with elevated VEGF level and poor prognosis in hepatocellular carcinoma. *Mod Pathol*. 2005;18(5):663–672.
40. Musso O, Rehn M, Théret N, et al. Tumor progression is associated with a significant decrease in the expression of the endostatin precursor collagen XVIII in human hepatocellular carcinomas. *Cancer Res*. 2001;61(1):45–49.
41. Quélard D, Lavergne E, Hendaoui I, et al. A cryptic frizzled module in cell surface collagen 18 inhibits Wnt/beta-catenin signaling. *PLoS One*. 2008;3(4):e1878.
42. Lavergne E, Hendaoui I, Coulouarn C, et al. Blocking Wnt signaling by SFRP-like molecules inhibits in vivo cell proliferation and tumor growth in cells carrying active β-catenin. *Oncogene*. 2011;30(4):423–433.
43. Walia A, Yang JF, Huang YH, Rosenblatt MI, Chang JH, Azar DT. Endostatin's emerging roles in angiogenesis, lymphangiogenesis, disease, and clinical applications. *Biochim Biophys Acta*. 2015;1850(12):2422–2438.
44. Poluzzi C, Iozzo RV, Schaefer L. Endostatin and endorepellin: A common route of action for similar angiostatic cancer avengers. *Adv Drug Deliv Rev*. 2016;97:156–173.
45. Ham J, Costa C, Sano R, et al. Exploitation of the apoptosis-primed state of MYCN-amplified neuroblastoma to develop a potent and specific targeted therapy combination. *Cancer Cell*. 2016;29(2):159–172.
46. Sarosiek KA, Fraser C, Muthalagu N, et al. Developmental regulation of mitochondrial apoptosis by c-Myc governs age- and tissue-specific sensitivity to cancer therapeutics. *Cancer Cell*. 2017;31(1):142–156.